JOURNAL OF MATERIALS SCIENCE 29 (1994) 1045–1050

Microstructure study of Sm, Mn-modified $PbTiO_3$ piezoelectric ceramics by XRD profile-fitting technique

ZENG YANWEI*, XUE WANRONG
Department of Silicates Engineering, Nanjing Institute of Chemical Technology, Nanjing 210009, People's Republic of China
A. BENEDETTI, G. FAGHERAZZI
Department of Physical Chemistry; University of Venice, Venice 30123, Italy

By using the X-ray diffraction profile-fitting technique, the microstructures of Sm, Mn-modified $PbTiO_3$ piezoelectric ceramic discs, including ferroelectric domain sizes, microstrains, and their variations with the poling strength have been quantitatively investigated. The results manifest that the modified $PbTiO_3$ ceramics contain a high density of domain walls due to the presence of finely-divided coherent domain structures (tens of nanometres in dimension). The poling treament can evidently influence the domain-size distribution, with a more homogeneous microstructure being developed; however, it simultaneously causes high anisotropic microstrains within the structure which, together with the high density of domain walls, is expected to be responsible for the unusual high electromechanical coupling properties possessed by this material.

1. Introduction

Modified $PbTiO_3$ is one of a few remarkable piezoelectric ceramic materials. Since the 1980s a lot of research effort has been devoted to developing and improving its ultra-high anisotropy in electromechanical coupling factors and piezoelectric coefficients, which make modified $PbTiO_3$ ceramics extremely useful in a wide range of applications such as high-frequency linear array transducers, SAW devices, infrared sensors, etc. [1–3]. One tailors materials, on the one hand, by incorporating various minor elements into the $PbTiO_3$ lattice, such as alkaline earths, rare earths, and transition elements, with the purpose of achieving (i) high Curie temperature, (ii) small dielectric constant, (iii) low Poisson's ratio, (iv) ultra-high electromechanical anisotropy ($K_t \gg K_p$) as well as (v) good stability at high frequency [4–8]. On the other hand, many researchers put their emphasis on exploring the reasons why this kind of material has such unusual properties. Arlt *et al.* [9] have suggested that there are at least two relaxing mechanisms that could make additional contributions to the piezoelectric coefficients of modified $PbTiO_3$ materials, one being closely associated with 90° domain wall movements, electronic and ionic defects, the other one mainly related to intrinsic properties of the materials like, the large axial ratio c/a.

Cross *et al.* [10] speculated that non-intrinsic negative contributions to the intrinsic d_{31} could lead d_{31} nearly to zero and even to a minus quantity, as observed in the piezoelectric polymeric materials [11] or some single-crystal materials [12]. In addition, Takashi *et al.* [6] attributed the high electromechanical anisotropy to the particular ionic radii of the doping rare earths, whereas Mendiola *et al.* [13] claimed that free PbO on the grain boundaries of sintered modified $PbTiO_3$ discs could facilitate 90° domain rotations during poling treatment, and hence yield an unusually large K_t/K_p.

However, so far, the mechanism that is responsible for the ultra-high electromechanical anisotropy possessed by modified $PbTiO_3$ is still a question open to study although many ideas have been proposed, as partly mentioned above. One especially still lacks a clear understanding of the electromechanical properties of modified $PbTiO_3$ from an insight into the microstructure of the material. The authors [14] have studied the 90° domain switching behaviour under various poling fields by carefully analysing X-ray diffraction (XRD) intensities of the materials. In the present work, microstructural information, including ferroelectric domain sizes, microstrains, and their variations with the poling strength, has been quantitatively investigated with Sm, Mn-modified $PbTiO_3$ ceramic discs by the XRD profile-fitting technique, in an attempt to narrow and bridge the gap between the electromechanical properties of modified $PbTiO_3$ materials and their microstructures.

* Responsible author to whom correspondence should be addressed. *Present address*: Applied and Industrial Chemistry Institute, University of Trieste, Via A. Valerio, 2-34127 Trieste, Italy.

0022–2461

2. Experimental procedure

2.1. Specimens and WAXS set-up

Three well-sintered specimen discs were selected for use in this study, which were nominally of the stoichiometry $(Pb_{0.85}Sm_{0.10})(Ti_{0.98}Mn_{0.02})O_3$. One specimen was unpolarized, labelled PTO1 in the present paper. The other two were subjected to moderate and full polarization at d.c. electric fields of 3 and 6 kV mm^{-1} and labelled PTO2 and PTO3, respectively.

Wide-angle X-ray scattering (WAXS) measurements of all three specimens were conducted on a Philips vertical goniometer connected to a highly stabilized generator. Ni-filtered CuK_α radiation, obtained from a Cu X-ray tube working at 45 kV and 30 mA, was employed together with a graphite monochromator, proportional counter and a pulse-height discriminator. The scattering profiles were registered in a step-by-step mode at interval 0.05° over an angular range from 10 to 120° in scattering angle 2θ.

2.2. Methodology used for microstructure information

In the present work the Warren–Averbach (W–A) method [15, 16] for microstructure analyses has been adopted. As early as the 1950s it was manifested that the Fourier transform $A(L)$ of diffraction profiles broadened due to micro-distortion of the lattice and smallness of coherent crystallite size can be written exactly as a product of the so-called size coefficient $A_s(L)$ and distortion coefficient $A_d(L)$:

$$A(L) = A_s(L)\,A_d(L) \quad (1)$$

and at sufficiently small L (a variable in real space) the logarithm of $A(L)$ can be given by

$$\mathrm{Ln}[A(L)] = \mathrm{Ln}[A_s(L)] - \frac{2\pi^2\langle e^2(L)\rangle L^2}{d_{(hkl)}^2} \quad (2)$$

where A_s is independent of the order of diffraction, while A_d depends upon the order; hkl are the Miller indices, $d_{(hkl)}$ is the interplanar spacing and $\langle e^2(L)\rangle$ the squared microstrain averaged over all distances L. According to Equation 2, therefore, in a plot of $\ln[A(L)]$ versus $1/d_{(hkl)}^2$ the slopes will directly give the lattice-distortion information $\langle e^2(L)\rangle$, and the intercepts at $1/d_{(hkl)}^2 = 0$ give the coherent crystallite size effects if multiple orders of diffraction in the same crystallographic plane family are experimentally available. The size effect $A_s(L)$ is associated with the volume-weighted domain-size distribution in the direction perpendicular to (hkl) planes by the relation:

$$Pv(L) \propto \frac{L\mathrm{d}^2[A_s(L)]}{\mathrm{d}L^2} \quad (3)$$

and hence the volume-weighted average domain size $\langle D\rangle_v$ can be calculated from

$$\langle D\rangle_v = \frac{\int_0^\infty LPv(L)\mathrm{d}L}{\int_0^\infty Pv(L)\mathrm{d}L} \quad (4)$$

Nevertheless, it should be pointed out that before W–A extraction of microstructure information it is most important to obtain, from the experimentally measured diffraction curve, structure-related diffraction profiles in which no instrumental broadening effects are involved. In order to do that, a convolutive profile-fitting procedure [17] is made use of, where a pseudo-Voigt function defined by Wertheim *et al.* as

$$pV(x) = I_p[yG(x) + (1 - y)C(x)] \quad (5)$$

has been used to convolute with the instrument function calibrated by a well-crystallized α-quartz specimen, and then directly fitted to the experimental peaks. In Equation 5, significant profile parameters are included: $C(x) = (1 + x^2) - 1$ and $G(x) = \exp[-(\ln 2)x^2]$ with $x = (2\theta - 2\theta_0)/w$; $2\theta_0$ is the $K_{\alpha1}$ peak maximum position, $2w$ the full width at half maximum of the total $K_{\alpha1}$ or $K_{\alpha2}$ profile, y the Gaussian content of the pV function and I_p the intensity at the $K_{\alpha1}$ peak maximum.

3. Results and discussion

3.1. Crystallographic structures

In order to detect the influence of poling treatment on the crystallographic structure, the directly-obtained XRD profiles of three specimens were first treated by the Rietveld whole-pattern-fitting technique under the space group P4/MMM. As an example, the plot output from Rietveld analysis of an unpoled $PbTiO_3$ disc specimen is illustrated in Fig. 1. The square root of residual errors (as goodness-of-fit) has arrived at a fairly good value (1.5). For the other two poled specimens, almost the same goodness-of-fit values have also been reached. Despite the fact that the whole-pattern-fitting results appear not to be excellent everywhere, mainly due to over-simplified mathematical treatment of the strong preferential orientation in the specimens, the Rietveld analyses definitely indicate that poling treatments do not damage the specimen's crystallographic structure, with no changes observed in their atomic coordinates and cell dimensions ($a = 0.39041 \pm 2.0 \times 10^{-5}$ nm, $c = 0.40720 \pm 6.0 \times 10^{-6}$ nm) for all three specimens. This conclusion is

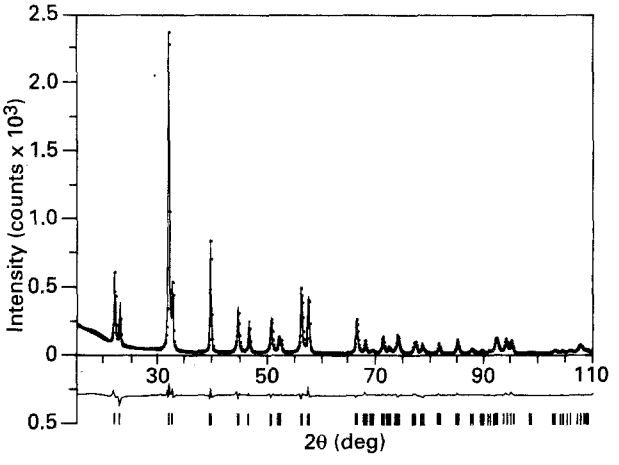

Figure 1 Rietveld-fit plot output for unpoled Sm, Mn-modified $PbTiO_3$.

consistent with that reported by Zeng *et al.* [14]. In addition, the Rietveld analyses allow all the reflections to be strictly indexed under space group P4/MMM and thus avoid some Miller-indexing mistakes possibly caused if referring only to the JCPDS data [18], which is very important for the subsequent profile-broadening analysis.

3.2. XRD profile-broadening analysis

The W–A analysis of profile broadening for microstructure information was selectively carried out on the reflection groups 0 0 1–0 0 2–0 0 3, 1 0 0–2 0 0–3 0 0 and 1 1 1–2 2 2, with the interest limited to three major crystallographic directions. Starting from the Fourier transform of the best-fitted profiles, the distributions of domain size and microstrain in the three above-mentioned directions for all the three specimens have been derived with W–A method and are illustrated below in Figs 2 and 3, respectively. In Table I some important characteristic values of these microstructure parameters are listed.

3.2.1. Domain sizes on average and their distribution

From the average values of domain size given in Table I, it can be seen that the ferroelectric domains in the modified-$PbTiO_3$ discs have the sizes predominantly of the order of magnitude of tens of nanometres. Those results seem to allow us to be aware that the crystalline grains in the modified-$PbTiO_3$ discs are highly divided by a large number of domain walls. In the [0 0 1] direction, particularly, such a division appears to be much stronger than in other directions, so that the domain sizes in the [0 0 1] direction are evidently smaller than those in the [1 0 0] direction, which makes the domains geometrically featured by flat shapes on the average. With such a picture of domain microstructure, it should be said that the modified-$PbTiO_3$ discs are actually a kind of domain-wall-intensive material, in which the additional contributions from domain-wall movements to the material's properties are supposed to be non-negligible.

TABLE I Microstructure parameters derived via W–A method for Sm, Mn-$PbTiO_3$ discs

Specimen	Direction [*hkl*]	Domain size (nm)[a]		Microstrain $\langle e^2\rangle^{1/2}$ at $\langle D\rangle_v/2$
		$\langle D\rangle_s$	$\langle D\rangle_v$	
PTO1	0 0 1	13.5	25.8	2.2×10^{-3}
	1 0 0	30.4	39.5	2.3×10^{-3}
	1 1 1	36.8	62.6	1.1×10^{-3}
PTO2	0 0 1	12.9	21.8	2.9×10^{-3}
	1 0 0	20.6	37.6	2.5×10^{-3}
	1 1 1	35.1	60.5	9.6×10^{-4}
PTO3	0 0 1	13.2	21.7	3.3×10^{-3}
	1 0 0	22.2	35.5	2.7×10^{-3}
	1 1 1	34.7	58.5	9.5×10^{-4}

[a] $\langle D\rangle_s$ is the surface-weighted average domain size in the direction [*hkl*] and $\langle D\rangle_v$ the volume-weighted average domain size.

The impact of poling treatment on the average domain sizes can be also discovered from Table I. A decrease of about 15% in average domain sizes took place when the discs were subjected to only a moderate poling treatment, but a less evident further decrease was observed as the poling field further increased. This fact seems to mean that the poling treatments cannot exert a steadily strong influence on the microstructure of domains. To a large extent, the poled modified-$PbTiO_3$ discs maintain the domain structures that have been established upon the fulfilment of the phase transition from cubic to tetragonal at the Curie point (about 500 °C). As a matter of fact, the fine domainization of crystalline grains, which may happen in company with the c–t transition of the material, provides an effective way to disperse and dissipate the distortion energy caused by the large change in volume (0.5%) and in shape ($c/a = 1.043$), and thereby to ensure the whole sintered discs of enough mechanical strength.

As illustrated in Fig. 2, furthermore, the domain size distributions in various directions show changes

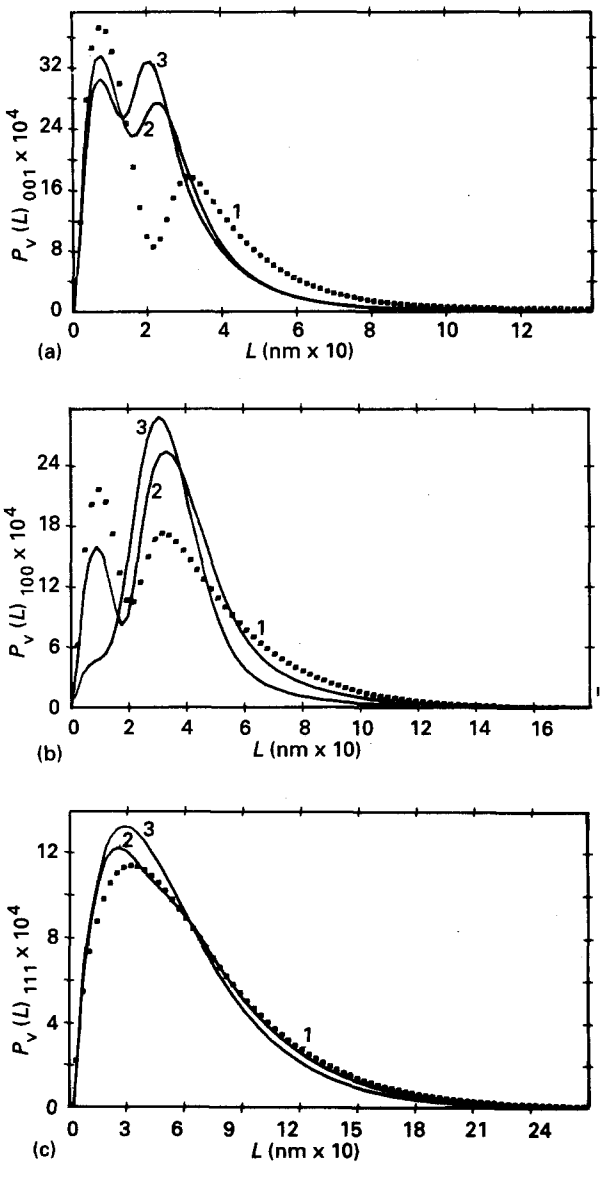

Figure 2 Domain-size distributions $P_v(L)$ in various directions: (a) [001], (b) [100], (c) [111]. (1) PTO1, (2) PTO2, (3) PTO3.

of domain microstructure in detail which seem to be hardly observed from just the averaged domain size values, but actually occur during the poling treatment. It is found that the domain sizes in the [0 0 1] and [1 0 0] directions for the three specimens all exhibit bimodal distributions. As the poling field force increases, the relative heights of the double distribution peaks are changed, with the result of enhancing the component of the domains of larger sizes but, at the same time, accompanied by a peak position shift towards the low end, i.e. a net decrease in total average size.

This is an interesting revelation of the modified-$PbTiO_3$ disc microstructure, viewed at a scale of tens of nanometres. The bimodal pattern of domain size distributions suggests that non-poled modified-$PbTiO_3$ discs can be structurally thought of as an assembly packed with some smaller domains (centred around 10 nm) and some larger domains (centred around 30 nm). It is speculated that the larger domains may arise from the domainization of smaller crystalline grains, while the smaller domains are produced from those larger grains that may account for about half of the total grains, since the c–t transition of a larger grain will creat large anisotropic stresses against its constrained surroundings so that a higher degree of twinning process would be needed to help dissipate the strain energy and eliminate the anisotropic stresses. In this sense, therefore, bimodal distributions of domain sizes may correspond in nature to two different degrees of twinnings driven by c–t transition. By the same principles it is also expected that the twinning process will mainly boost 90° rather than 180° domains within the sintered discs, since the formation of 90° domains is favourable to lessening the anisotropic strains on the whole.

To understand the changes under poling fields of the domain microstructure portrayed above, the following interpretation appears to be physically sound. For any one couple of 90° domains, the partner domain that has an unfavourable spontaneous polarization vector with respect to the poling field will be necessarily compelled to change its effective spontaneous polarization vector to an extent depending on the applied poling force. It is believed that such a change could be accomplished through two mechanisms: one is the shifting of domain walls towards the unfavoured partner domain, with the other partner domain volume growing. Obviously, this process will increase the anisotropic strains in the materials, but with no new domain walls introduced and even with partial extinction of the existing domain walls. The other mechanism is further twinning in the unfavoured partner domains, which produces new domain walls, but the anisotropic strains in the materials are expected to be reconciled to a better spatial fit compared with the case governed by the domain-wall-shifting mechanism. Therefore, by viewing the variation of domain size distributions with poling treatment as shown in Fig. 2, it follows that the first mechanism seems to function predominantly in the smaller domain pairs, while the second mechanism might work mainly with the larger domain pairs. This inference is consistent with the fact that the component of smaller domains goes down and the component of larger domains goes up, but the mean values of larger domain sizes show an evident decrease as the poling field force increases. It is sure that under the poling field force, the enlargement of small-sized domains towards the energy-favourable polarization direction and the further twinning of unfavoured large-sized domains will endow the materials with an apparent macro-polarization, and simultaneously make the domain sizes distribute more homogeneously. To some extent, the latter could be beneficial to the structure conservation and mechanical strength of the materials.

By comparing the domain size distributions in the various directions, it is easy to find that the size distributions in [1 0 0] and [0 0 1] both show bimodal patterns but differ a lot from each other in detail, while a normal monomodal size distribution was only found in the [1 1 1] direction, as demonstrated in Fig. 2c. Unfortunately, it seems to be rather hard to establish a quantitative correlation among the domain size distributions in different directions, but it is believed that these results are closely associated with the particular configurations of mutually coupled 90° domains.

3.2.2. Microstrains and their distribution

As defined in the W–A method, the microstrain $\langle e^2(L)\rangle^{1/2}$ is an averaged quantity over all the distances of length L within the coherent domains. The microstrain $\langle e^2(L)\rangle^{1/2}$ is therefore actually a function of the statistical length L. When L is small, $\langle e^2(L)\rangle^{1/2}$ reveals the local distortions in the crystal lattice, whereas it gives information on averaged distortion at a large scale when L takes a large value.

Fig. 3 illustrates microstrain variations in the [0 0 1] direction, whose microstrain distribution specimens. It is found that all the microstrain distribution curves have a nearly perfect hyperbolic trend in the $\langle e^2(L)\rangle^{1/2}$ versus L plot, similar to curves 2 and 3 in Fig. 3, except for the unpoled specimen in the [0 0 1] direction whose microstrain distribution, (curve 1 in Fig. 3) first shows an increase but is subsequently followed by a decrease with a plateau in the intermediate range. According to the theory of Rothman and Cohen [19] and others, the hyperbola-like microstrain distribution can be interpreted as due

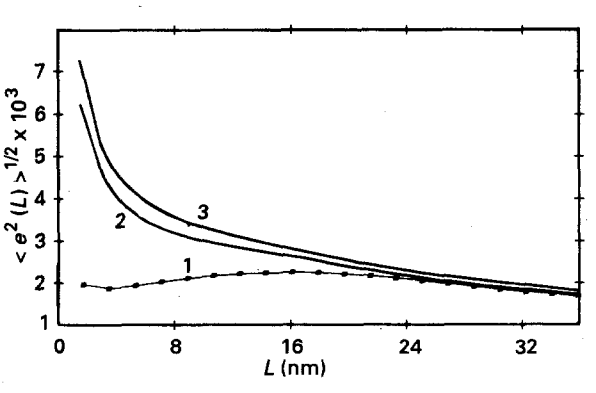

Figure 3 Microstrain distributions $\langle e^2(L)\rangle^{1/2}$ in the direction [001] for three specimens: (1) PTO1, (2) PPO2, (3) PTO3.

to the presence of intracrystalline disorder caused by dislocations inside coherent domains; while from the theory of Crist and Cohen [20] and others, the unpoled specimen's microstrain distribution in the [0 0 1] direction is supposed to be attributed to a lattice parameter fluctuation which reflects the inhomogeneity of the microstructure. As a speculation, here the microstructural inhomogeneity may be related in nature to the highly bimodal distribution of domain sizes, and the intracrystalline disorder may be ascribed to the results of poling treatment. Undoubtedly the relative magnitudes of the microstrains at a particular length L definitely describe the degree to which microstructural disorder is involved in this material.

In the last column of Table I, the magnitudes of the microstrains at half the averaged domain sizes (volume-weighted) are given. It can be seen that at such a length scale, the averaged microstrains in the [0 0 1] and [1 0 0] directions both show an evident increase as the poling force is raised. With respect to the unpoled specimen, moreover, the microstrain increment of the fully poled one amounts to as much as 50% in the [0 0 1] direction, much higher than the 17% increment in the [1 0 0] direction. In contrast, the microstrain in the [1 1 1] direction exhibits somewhat of a decrease. This information clearly indicates that the poling process, which stimulates 90° domains to "switch" and creats apparent macro-polarization of the specimens, enhances the anisotropic microstrains in the materials, despite the readjustment of domain-size distributions that are expected to be very important for the relaxation of interior structural anisotropy. Nevertheless, what is more significant may be that this analytical result remind us to correlate them with the origin of the high electromechanical coupling properties possessed by this kind of material.

For a simple discussion, a modified-$PbTiO_3$ ceramic disc fully poled along the axial direction is substituted by a piece of equivalent piezoelectric body of symmetry C_∞, whose macro-polarization direction is approximately viewed as parallel to [0 0 1] of the modified $PbTiO_3$ lattice due to the strongly preferential orientation of the domains after the poling treatment; and the modified-$PbTiO_3$ material is supposed to have an isotropic stress–strain property schematically represented by Fig. 4. As a matter of fact, the anisotropic microstrains inside the disc imply that the equivalent piezoelectric body will work in an anisotropic stress state if an alternating signal is applied to it. With reference to the stress–strain property in Fig. 4, a higher stress (or strain) in the axial direction will correspond to a lower elastic compliance in the same direction, and in the radial direction a higher compliance will be expected due to the lower stress. Therefore the anisotropic microstrains practically make the material apparently exhibit much "harder" properties in the axial direction than in the radial direction. As a result, it will necessarily cause a stronger axial electromechanical coupling compared with that in the radial direction. From the above simple discussion, it can be concluded qualitatively that the microstrain anisotropy in modified $PbTiO_3$ should be responsible,

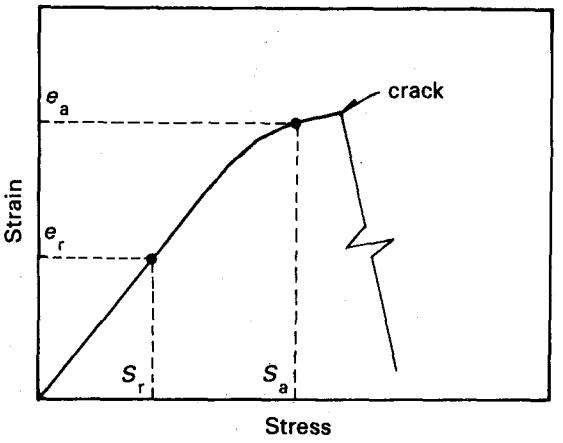

Figure 4 Schematic stress–strain property diagram of the modified $PbTiO_3$.

at least partially, for the high electromechanical anisotropy possessed by this material. Nevertheless, the somewhat coincidental achievement of high microstrain anisotropy and sufficient mechanical strength in the material is supposed to be a composite result of many complicated factors such as high crystallographic axial ratio c/a, reasonable domain-size distribution, appropriate domain interface energy, and so on. Some of them may depend only on the material chemistry, but some may be delicately associated with the details of the material preparation.

4. Conclusions

In summary, the XRD profile-analysing method provides an efficient approach to unveiling microstructural details of the ferroelectric domains in sintered modified-$PbTiO_3$ materials and their variations with poling treatment. From the present research work, the following significant conclusions can be drawn:

1. The average domain sizes in different directions reveal that most of the domains are of several tens of nanometres in dimensions and are characterized by flat shapes in the [0 0 1] direction. The smallness of ferroelectric domains endows the material with a high domain-wall density, which may be expected to make non-negligible additional contributions to the material electromechanical constants.

2. A highly bimodal distribution of domain sizes was found in the unpoled $PbTiO_3$ specimen. It can be viewed as a kind of microstructural inhomogeneity present in the material. The poling treatment seems not to steadily influence the average domain sizes as the poling force increases, but it evidently changes the domain-size distribution with the result of making domain sizes distribute more homogeneously. It is believed that a more homogeneous dispersion of domain sizes will effectively relax part of the anisotropic strains caused by domain switching under the poling force.

3. The microstrain distributions of poled specimens all show a hyperbolic trend in the $\langle e^2(L)\rangle^{1/2}$ versus L plot, which can be attributed to the presence of intracrystalline disorder caused by dislocations inside the

domains. However, a non-hyperbola-like microstrain distribution has been observed in the [0 0 1] direction of the unpoled specimen, which has been tentatively interpreted as a reflection of microstructural inhomogeneity in terms of the theory of Crist and Cohen.

4. The microstrains at half average domain size show a strong dependence on the poling treatment. In the [0 0 1] direction, the microstrain increment in the fully poled specimen increases by 50% in comparison with the unpoled one, whereas in the other two directions a much smaller increment and even somewhat of a decrease in the microstrains have been observed. This result reveals that the poling treatment can result is highly anisotropic microstrains in the modified-$PbTiO_3$ disc, so that the disc may behave as being much "harder" in the axial direction than in the radial direction. It is therefore considered that such a highly anisotropic microstrain must also be one of the important factors responsible for the high electromechanical anisotropy of the materials.

References

1. H. HONDA, Y. YAMASHITA and K. UCHIDA, in Proceedings of IEEE Utrasonics Symposium, IEEE Press (1982) p. 845.
2. Y. ITO, H. TAKEUCHI, K. NAGATSUMA, S. JYOMURA and S. ASHIDA, *J. Appl. Phys.* **52** (1981) 3223.
3. N. ICHINOSE, *Amer. Ceram. Soc. Bull.* **64** (1985) 1581.
4. Y. YONKACHI *et al.*, *Jpn J. Appl. Phys.* **11** (1981) L241.
5. Y. YAMASHITA *et al.*, *ibid.* **20** Suppl. 20/4 (1981) 183.
6. TAKASHI *et al.*, *Ferroelectrics* **54** (1984) 131.
7. H. TAKRUCHI, H. TAKEUCHI, S. JYOMURA, E. YAMAMOTO and Y. ITO, *J. Acoust. Soc. Amer.* **72** (1982) 1114.
8. W. R. XUE *et al.*, *Jpn J. Appl. Phys.* **24** Suppl. 24/2 (1985) 718.
9. G. ARLT and H. DEDERICHS, *Ferroelectrics* **29** (1980) 47.
10. L. E. CROSS *et al.*, in Proceedings of IEEE Ultrasonics Symposium (1986) p. 637.
11. E. FUKADA, *Ferroelectrics* **60** (1984) 285.
12. T. YAMAGNCHI and K. HAMANO, *J. Phys. Soc. Jpn* **50** (1981) 3956.
13. J. MENDIOLA, M. L. PARDO and L. D. OLMO, *Ferroelectrics* **79** (1988) 1249.
14. Y. W. ZENG, W. R. XUE and G. F. FU, *J. Mater. Sci.* **26** (1991) 4293.
15. B. E. WARREN and B. L. AVERBACH, *J. Appl. Phys.* **21** (1950) 596.
16. *Idem, ibid.* **23** (1952) 1059.
17. S. ENZO, G. FAGHERAZZI and A. BENEDETTI, *J. Appl. Crystallogr.* **21** (1988) 536.
18. JCPDS Power Diffraction File 6-0452.
19. R. L. ROTHMAN and J. B. COHEN, *J. Appl. Phys.* **42** (1971) 971.
20. B. CRIST and J. B. COHEN, *J. Polym. Sci.* **17** (1979) 1001.

Received 30 March
and accepted 24 August 1993